H-infinity controller design for active magnetic bearings considering nonlinear vibrational rotordynamics

Matthew O. T. COLE*, Chakkapong CHAMROON** and Patrick S. KEOGH***

*Department of Mechanical Engineering, Chiang Mai University,
239 Huay Gaew Rd, Chiang Mai 50200, Thailand.
E-mail: motcole@hotmail.com

**Dept. of Mechanical Engineering, University of Phayao
19 Maeka, Phayao 56000, Thailand.

***Department of Mechanical Engineering, University of Bath,
Bath BA2 7AY, UK.

Abstract

This paper deals with optimal controller design for active magnetic bearing (AMB) systems for which nonlinear rotordynamic behavior is evident, and so vibration predicted by operating point linearization differs substantially to that which actually occurs. Nonlinear H-infinity control theory is applied with a rotordynamic model involving nonlinear stiffness and/or damping terms. The associated Hamilton-Jacobi-Isaacs (HJI) equation is formulated and solved to obtain a state feedback control law achieving specified vibration attenuation performance in terms of the peak L_2 gain of the nonlinear system. The method is applied in case study to a flexible rotor/AMB system that exhibits nonlinear stiffness properties owing to rotor interaction with a clearance bearing. Simulations are performed to quantify RMS vibration due to harmonic disturbances and the results compared with the norm-bound values embedded in the HJI equations. A feedback controller design method is then presented that is similar in approach to the standard loop-shaping/mixed-sensitivity methods used for linear systems, and involves augmenting the system model with weighting transfer functions. Experiments are undertaken to compare controller performance for design based on nonlinear and linearized models. The results highlight the shortcomings of applying linear optimal control methods with rotor systems exhibiting nonlinear stiffness properties as large amplitude vibration and loss of rotordynamic stability can occur. Application of the described nonlinear H-infinity control method is shown to overcome these problems, albeit at the expense of vibration attenuation performance for operation in linear regimes.

Keywords : rotor vibration, magnetic bearings, H-infinity control, nonlinear dynamics

1. Introduction

The successful application of modern optimal and robust control methodologies with AMB/rotor systems has been widely reported. For frequency domain analysis and design, industry standards have now been established that fit well within the framework of linear H-infinity control (Schweitzer and Maslen, 2010). In this framework, specifications for rotor vibration attenuation are defined using system norm-bound criteria, which can directly account for external disturbances having specified sources and spectral characteristics, e.g. sensor noise, rotor unbalance and external motions. The limitations of a linear design may be exposed, however, when large amplitude vibration occurs, or when the rotor equilibrium position varies significantly during operation, as nonlinear effects can then become important.

Previous works on active control of vibration in nonlinear rotordynamic systems cover quite diverse aspects. Unbalance compensation for a single-disk rotor with nonlinear supports was considered by Inoue et al. (2009). Control of synchronous vibration for a rotor supported by magnetic bearings when contacting with clearance bearings was investigated by Cole and Keogh (2003) and Chamroon et al., (2014), while active clearance bearings have also been proposed for a similar purpose in (Cade et al., 2010). In other work, destabilizing nonlinear effects have been accounted for in controller designs via linear approximations (Simon and Flowers, 2008, El-Shafai and Dimitri 2010, Karkoub,

2011). Nonlinear H-infinity control methods have been applied previously with magnetic bearings to deal with nonlinear properties of the AMBs (rather than rotordynamics) as, for example, by Sinha and Pechov (2005).

According to standard definitions, an optimal H-infinity controller for a nonlinear system achieves a minimum value for the peak RMS gain, i.e. minimizes the induced L_2 to L_2 norm of the closed loop system. The solution can be found by solving a partial differential equation known as the Hamilton-Jacobi-Isaacs (HJI) equation (Van der Schaft, 1992, Isidori and Alstofi 1992). This is usually a difficult task, due to nonlinearity of the HJI equation and non-uniqueness of the solution in the suboptimal case. It is shown here that, for rotordynamic models incorporating nonlinear stiffness and/or damping effects, a solution to the HJI equation (in inequality form) can be obtained by numerical optimization if a certain form of Lyapunov function is adopted. The main aim of this paper is to investigate whether the obtained solutions are practically useful for enhancing vibration suppression qualities of AMB control for rotors that exhibit significant nonlinear dynamic behavior.

2. Nonlinear rotordynamic model

Vibration of a nonlinear rotordynamic system subject to disturbance forces d and magnetic bearing control forces u, applied directly to the rotor, may be described by a matrix equation of the form

$$M\ddot{s} + G\dot{s} + Ks = E_f f(s,\dot{s}) + E_u u + E_d d \tag{1}$$

The vector f comprises a set of internal forces that vary as nonlinear functions of a subset of velocity and/or displacement states, which will be denoted z. Defining the state vector $x^T = [s^T\ \dot{s}^T]$, a state space representation is

$$\dot{x} = Ax + B_f f(z) + B_d d + B_u u \tag{2}$$

$$z = Cx \tag{3}$$

$$A = \begin{bmatrix} 0 & I \\ -M^{-1}K & -M^{-1}G \end{bmatrix},\ B_u = \begin{bmatrix} 0 \\ M^{-1}E_u \end{bmatrix}, B_d = \begin{bmatrix} 0 \\ M^{-1}E_d \end{bmatrix}, B_f = \begin{bmatrix} 0 \\ M^{-1}E_f \end{bmatrix} \tag{4}$$

A linearized model for the equilibrium point $x = 0$ is given by Eq. (2) with $f = 0$. For the purpose of controller design, it is appropriate to further define a set of output variables for inclusion in a cost function. These may be expressed as a linear function of x and u:

$$y = C_y x + D_u u \tag{5}$$

3. Existence of H-infinity controllers

The peak L_2 gain for a nonlinear system described by Eqs (2)-(5) may be defined as

$$Peak\ Gain_{L_2} = \sup_{d\neq 0} \frac{\|y\|_2}{\|d\|_2} \tag{6}$$

where $\|.\|_2$ denotes the signal L_2-norm: $\|y\|_2 = \left(\int_{-\infty}^{\infty} y(t)^2 dt\right)^{\frac{1}{2}}$. It is well known that for linear systems the peak L_2 gain is a time-domain version of the H-infinity norm. According to standard theory, under the assumptions $D_u^T C_y = 0$ and $D_u^T D_u = I$, if there exists a positive semi-definite function $V(x) \geq 0$ with bounded Jacobian $V_x(x) = dV/dx$ satisfying the Hamiltonian-Jacobi-Isaacs equation given by

$$V_x\left(Ax + B_f f(z)\right) + x^T C^T C x + \frac{1}{4}\gamma^{-2} V_x B_d B_d^T V_x^T - \frac{1}{4} V_x B_u B_u^T V_x^T = 0 \tag{7}$$

then, the control law $u = -\frac{1}{2}B_u^T V_x^T$ renders the controlled system stable with $Peak\ Gain_{L_2} < \gamma$ (Isidori and Astolfi, 1992). In general, it is difficult to solve Eq. (7) unless some further assumptions are made about the form of $V(x)$. Although methods based on multi-dimensional Taylor series expansions can be used (Sinha and Pechev, 2004, Abu-Khalaf et al., 2006), the numerical complexity for high order systems is prohibitive. In this study we adopt a quadratic Lyapunov function with additional higher order terms in the nonlinear variables z only:

$$V(x) = x^T P x + 2g(z) \tag{8}$$

where $P = P^T > 0$. Noting that $V_x = 2x^T P + 2\ g_z C$ where $g_z = dg/dz$, the HJI equation then becomes

$$x^T\left(PA + A^TP + C_y^TC_y\right)x + \gamma^{-2}x^TPB_dB_d^TPx - x^TPB_uB_u^TPx + 2g_z(z)CB_ff(z) + 2\left(f(z)^TB_f^TP + g_z(z)CA\right)x = 0 \quad (9)$$

Without any assumptions about the form of $f(z)$, the first three quadratic terms in x and remaining nonlinear terms must sum independently to zero. This requires that $CB_f = 0$ and $f(z)^TB_f^TP + g_z(z)CA = [0]$. By choosing

$$g_z(z) = f(z)^T\Sigma \quad (10)$$

equation (9) will hold if Σ and P satisfy

$$B_f^TP + \Sigma CA = [0] \quad (11)$$

$$PA + A^TP + C_y^TC_y + \gamma^{-2}PB_dB_d^TP - PB_uB_u^TP = [0] \quad (12)$$

A feasible solution (P, Σ) to these equations provides the control law

$$u = -\tfrac{1}{2}B_u^TV_x^T = -B_u^TPx - B_u^TC^T\Sigma^Tf(z). \quad (13)$$

To obtain a less conservative result, the constraint Eq. (11) can be relaxed if $f(z)$ is a scalar mapping and satisfies a sector bound condition:

$$f(z)(f(z) - \bar{\kappa}z) \le 0 \quad \Leftrightarrow \quad f(z) = \kappa(z)z, \;\; 0 \le \kappa(z) \le \bar{\kappa} \quad (14)$$

In this case, it is possible to reformulate the gain-bound condition Eq. (9) as a linear matrix inequality (LMI) that can be solved numerically. Given that Eq. (10) must still be satisfied, a sufficient condition for a solution to Eq. (9) to exist is that there exists P, Σ such that

$$x^T\left(PA + A^TP + C_y^TC_y + \gamma^{-2}PB_dB_d^TP - PB_uB_u^TP\right)x + 2f^T\Sigma CB_ff + 2f^T\left(B_f^TP + \Sigma CA\right)x < 0 \quad (15)$$

Equation (15) will hold for all scalar $f(z)$ satisfying Eq. (14) if there exists $P = P^T > 0$, Σ and $\mu > 0$ satisfying the following matrix inequality, as obtained by application of the so-called *S*-procedure (Boyd et al., 1994):

$$F(P, \Sigma, \mu) = \begin{bmatrix} A^TP + PA - PB_uB_u^TP & PB_f + A^TC^T\Sigma^T + C^T\bar{\kappa}\mu & PB_d & C_y^T \\ B_f^TP + \Sigma CA + \mu\bar{\kappa}C & -2\mu + \Sigma CB_f + B_f^TC^T\Sigma^T & 0 & 0 \\ B_d^TP & 0 & -\gamma^2I & 0 \\ C_y & 0 & 0 & -I \end{bmatrix} < 0 \quad (16)$$

To ensure $V(x) \ge 0$ we must also impose $P > 0, \Sigma \ge 0$. The controller is given by Eq. (13).

4. Vibration analysis and controller design for a flexible rotor

4.1 System description

The described nonlinear H-infinity control approach was applied to the experimental rotor-AMB system shown in Fig 1. The rotor is constructed from a steel shaft of length 700 mm and diameter 10 mm supported by ball bearings at each end. Two disks are fixed on the shaft. Disk 1 has mass 0.36 kg and forms the hub of the AMB. A backup bearing with radial clearance of 1 mm is also installed within the AMB. Disk 2, which has a mass 1.12 kg, is surrounded by a clearance ring which is compliantly supported by a force-sensing unit (stator unit). The radial clearance is 0.4 mm. Pairs of non-contact probes measure lateral displacement in orthogonal directions at both disks. The AMB was initially operated under PD feedback control. A linearized model was identified from frequency response measurements, which captures small-amplitude vibration behavior. Large amplitude vibration leads to contact interaction between disk 2 and the surrounding ring and this contributes a nonlinear stiffness effect on rotordynamic behavior. For a nominal rotational speed range of 0-200 rad/s, which includes the first critical speed, coupling between x-z and y-z planes is negligible. Models of rotor vibration under PD feedback control may be defined separately for each transverse plane in the form

$$\dot{x} = Ax + B_2f(z) + B_1d + B_1u \quad (17)$$

$$y = C_1x, \qquad z = C_2x \quad (18)$$

Subscripts here identify input/output matrices pertaining to disks 1 and 2: the disturbance force d and control input u both act at disk 1. Note that the control force u acts in addition to the feedback component from the PD controller, which is already accounted for in the model. The system output y is the rotor displacement at disk 1.

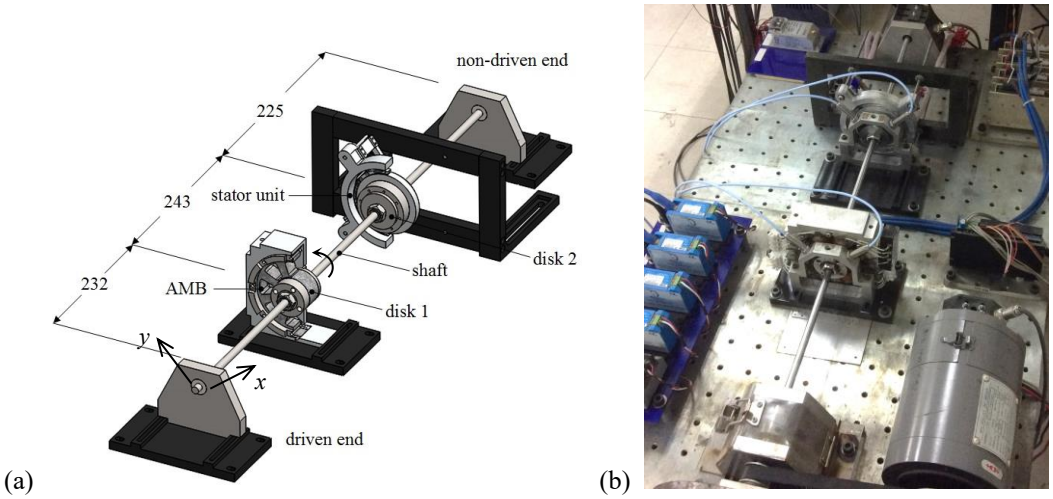

Fig. 1 Experimental flexible rotor-AMB system used in case study: (a) CAD model with cross section (b) photograph

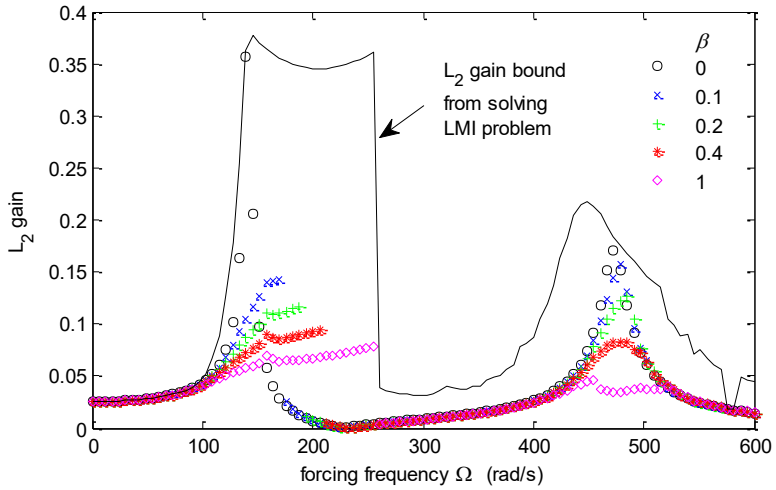

Fig. 2 L_2 gain calculated from simulation runs with harmonic forcing: results are shown for a selection of values for the non-linear parameter β. The peak L_2 gain-bound obtained by solving LMI problem Eq. (16) is also shown

The state vector x has four states which capture the first two natural modes of vibration of the rotor. This model has the form of Eqs (2)-(5) and so the control synthesis LMI Eq. (16) can be readily applied. Note that full state information is required to implement the controller and this is made possible by measurement of displacement at both disks, from which velocity states are calculated using a filtered derivative method.

4.2 Nonlinear vibration analysis via LMIs

Numerical simulations were performed using the model of the PD-controlled system with harmonic forcing at disk 1: $d = m_e\Omega^2 \cos\Omega t$. The exact characteristics of the rotor interaction with the clearance ring are uncertain and so, for theoretical investigation, a cubic nonlinear stiffness was adopted $f(z) = \beta\, z^3$. Time-step integration of Eq. (18) (with $u = 0$) was performed for a range of values of forcing frequency Ω and nonlinear parameter β. For each simulation run the L_2 gain was calculated as $\|y\|_2/\|d\|_2$. The results are shown as scattered points in Fig. 2. For the linear case ($\beta = 0$) the two resonant peaks are clearly evident and are associated with the first and second natural modes for lateral vibration of the flexible rotor. For larger values of β, constraining effects due to the nonlinear stiffness tend to reduce the amplitude of vibration but also extend the frequency range for resonance for the first natural mode. There are large disparities between the magnitude of vibration occurring in the linear and nonlinear cases for a frequency range 140-250 rad/s and it is this frequency range that will be a focus for controller design and testing.

For direct analysis, the system described by Eqs (17) and (18) is combined with an input weighting function, as shown in Fig. 3. The transfer function $W_1(s)$ is a stable approximation of the forcing function $\cos\Omega t$ given by

$$W_1(s) = \frac{2\zeta\Omega s}{s^2+2\zeta\Omega s+\Omega^2} \tag{19}$$

This resonant filter is used to probe the L_2 gain characteristics for harmonic forcing. If ζ is chosen sufficiently small then, for a stable linear system ($f = 0$), we have

$$Peak\ Gain_{L_2} = \sup_{\tilde{d}\neq 0} \frac{\|y_1\|_2}{\|\tilde{d}\|_2} = \left\|W_1(s)G_{yd}(s)\right\|_\infty = \sup_\omega \bar{\sigma}\left(W_1(j\omega)G_{yd}(j\omega)\right) \approx \bar{\sigma}\left(G_{yd}(j\Omega)\right) \tag{20}$$

For the nonlinear case, this frequency domain interpretation is no longer valid. Nonetheless, the value of the peak L_2 gain provides a useful bound on the magnitude of vibration (in the sense of the L_2 norm) under conditions of harmonic forcing. An upper bound on the value of the peak gain can be obtained by solving the LMI Eq. (17) with the smallest possible value of γ. Values for the peak-gain bound obtained by solving the LMI problem for a range of values of Ω are shown in Fig. 2. Note that for this analysis $B_u = 0$ as the PD controller is already accounted for within the model and no additional control is being applied. For the LMI analysis, the forcing amplitude is not accounted for directly but is implicit in the choice of $\bar{\kappa}$. Larger forcing amplitude is associated with larger values of $f = \beta\, z^3$ and hence, a larger value of $\bar{\kappa} = \sup_t\left(f(t)/z(t)\right) = \beta\sup_t(z(t)^2)$. For the results shown in Fig. 2, the LMI gain-bound was obtained using the actual value of $\bar{\kappa}$ from each simulation run. The gain-bound from the LMI analysis is seen to be sufficiently 'tight' to warrant its further application in the controller synthesis problem – which seeks to reduce the gain bound through application of an optimized feedback control law.

4.3 Robust feedback control synthesis

For controller synthesis, the augmented plant structure shown in Fig. 4 was considered. Here, the output weighting $W_1(s)$ reflects the expected characteristics of the disturbance signals (as for the analysis case in Fig. 3). Note that $W_1(s)$ is now applied at the output of the plant so that, for implementation, the states of $W_1(s)$ can be reconstructed from measurement of y. In the case study, we consider rotating unbalance as the main source of vibration excitation and seek to minimize vibration at disk 1 only. Hence, we may anticipate nonlinear behavior due to large amplitude vibration at disk 2. The weighting function W_1 is therefore chosen to penalize y over a frequency range corresponding to rotational speeds 0-200 rad/s, but emphasizing a nominal operating speed of 190 rad/s.

For linear controller design, the weighting function W_2 would be chosen so that $|W_2(j\omega)|$ exceeds the multiplicative uncertainty in the plant (frequency response) model. According to the small gain theorem, if the closed loop system model T_{ud} (from d to u) satisfies $\|W_2T_{ud}\|_\infty < 1$, the actual closed loop system will then always be stable. Strictly, these arguments are appropriate for linear systems only. Nonetheless, limiting the peak L_2 gain of the nonlinear system W_2T_{ud} helps to create a controller that is more robust to model error (although an appropriate choice of W_2 to guarantee stability is harder to deduce). The synthesis problem is to obtain a control law such that the peak L_2 gain of the closed loop system from d to $\tilde{y}$ is less than 1. This is a nonlinear version of an H-infinity control problem, similar to the mixed sensitivity design paradigm, with the objective to achieve a closed loop system satisfying

$$\left\|\begin{matrix} W_1T_{yd} \\ W_2T_{ud}\end{matrix}\right\|_\infty < 1 \tag{21}$$

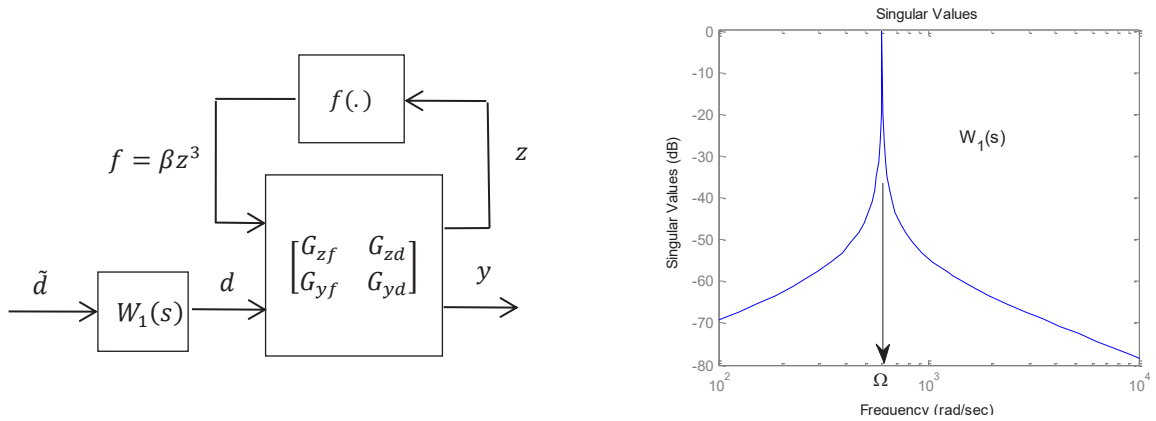

Fig. 3 The nonlinear rotordynamic model is augmented with a weighting function (disturbance model) for analytical determination of the L_2 gain under conditions of harmonic excitation

The controller solution will thereby provide vibration attenuation performance with robust stability. The state-space model for the augmented plant has the same form as Eqs (2)-(5) but with new state vector $\tilde{x}$, which combines the rotor states x with weighting function states x_1 and x_2 according to $\tilde{x}^T = [x^T \quad x_1^T \quad x_2^T]$, as shown in Fig. 4.

Figure 5 shows the frequency response characteristics (singular values) for the linearized closed loop dynamics T_{yd} and T_{ud}, together with the inverse of the weighting functions W_1^{-1} and W_2^{-1}. The inverse weighting functions exceed the maximum singular values over all frequencies, which is in agreement with Eq. (21). Hence, the required H-infinity performance and robustness properties are confirmed, at least for the linearized system.

5. Experimental results

Nonlinear H-infinity controllers were implemented and tested on the experimental system. For comparison, a linear H-infinity controller was designed based on the same formulation and a comparable choice of weighting functions. It was found that the linear H-infinity controllers generally had good vibration attenuation characteristics over a low frequency range (0-200 rad/s), even for nonlinear operation. This can be explained by the increased damping for the first flexural mode. However, for certain choices of W_1, closed loop stability was not maintained when rotor interaction with the clearance ring occurred at disk 2. In contrast, the nonlinear H-infinity controller was able to maintain stability over the full range of linear and nonlinear operating conditions. It thus became clear that, for linear controller design, stability under nonlinear operation was difficult to ensure and sensitive to the exact choice of weighting functions. So the approach of dealing with nonlinear effects explicitly was clearly advantageous.

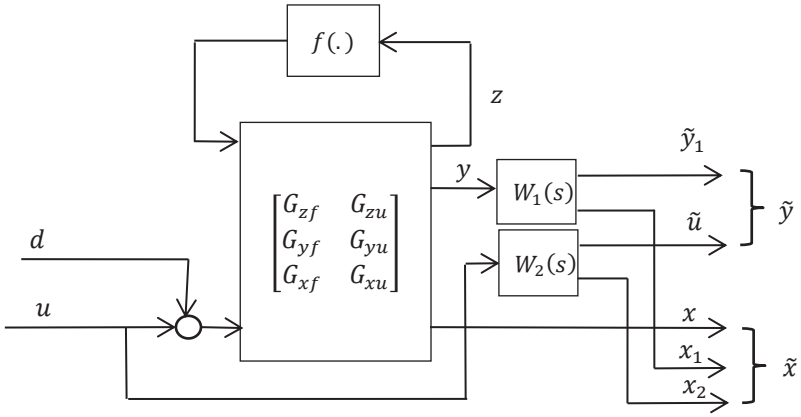

Fig. 4 Augmented plant for nonlinear H-infinity controller synthesis

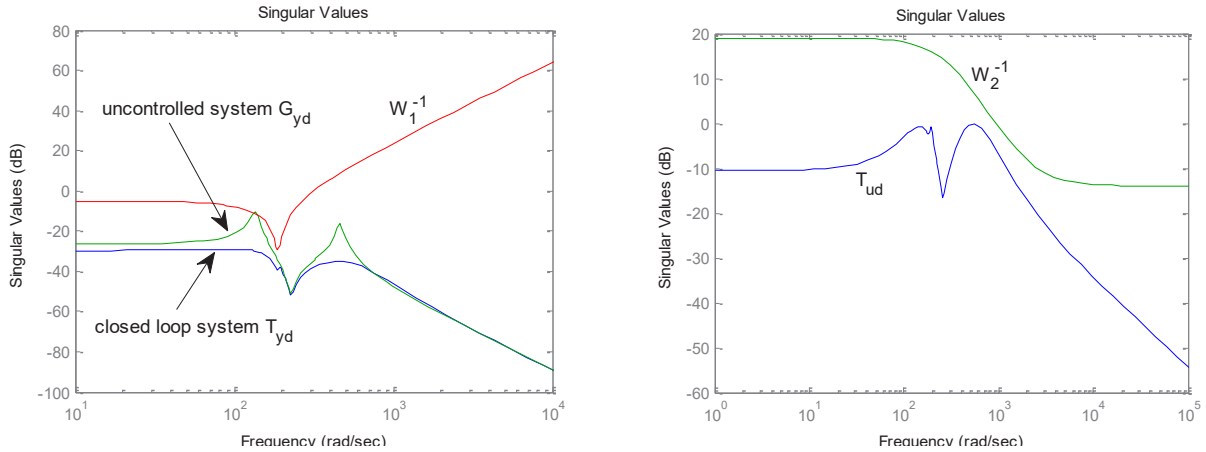

(a) (b)

Fig. 5 Results of nonlinear H-infinity controller design. Plots show frequency response characteristics for the linearized closed loop system: (a) vibration attenuation performance (b) robust stability

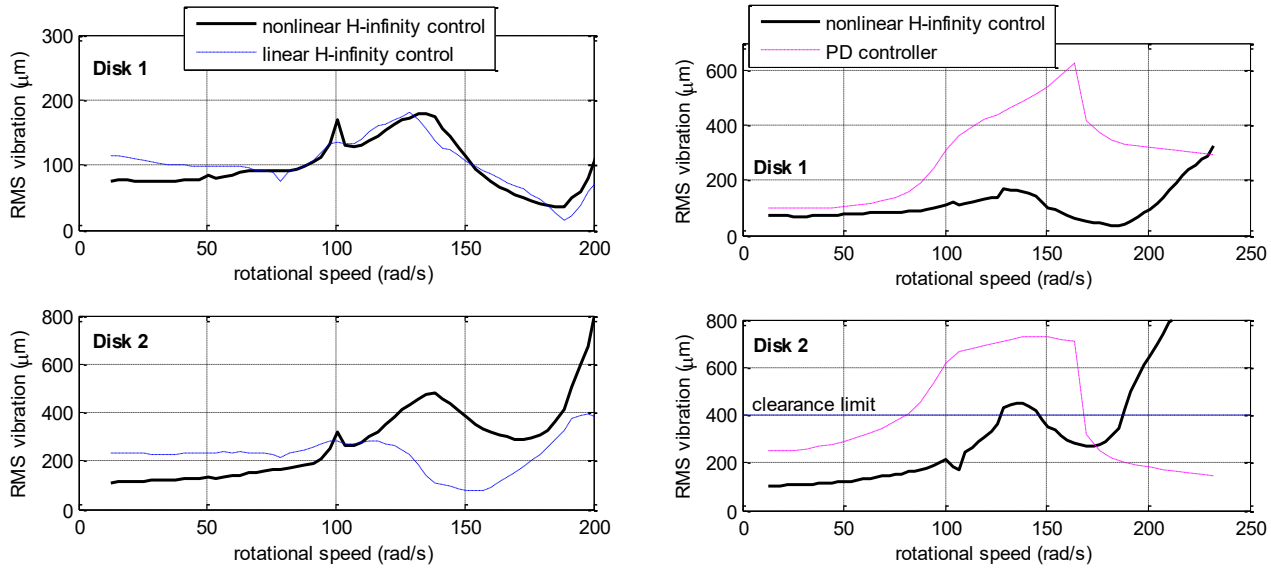

(a) linear operation (without clearance ring) (b) nonlinear operation (with clearance ring)

Fig. 6 Rotor vibration during steady speed rotation: (a) no rotor-stator contact interaction (linear case) (b) with rotor-stator contact interaction (nonlinear case)

Figure 6 shows rotor vibration levels for constant rotational speed, quantified in terms of the RMS displacements measured at disks 1 and 2. Figure 6a, shows results for both linear and nonlinear H-infinity designs under linear operation (with no clearance ring fitted). The controllers gave similar results in terms of RMS vibration at disk 1, although the linear controller design gave reduced vibration for the nominal operating speed of 190 rad/s. The response behavior reflects the overall form and scaling of W_1 (see Fig. 5a). The vibration at disk 2, which is not included in the cost function, is noticeably different for the two controllers. Figure 6b shows results for nonlinear operation, with installation of the clearance ring at disk 2. The nonlinear H-infinity controller was effective for the full range of running speeds and unbalance conditions tested. The unbalance condition of the rotor was such that hard interaction with the clearance ring only occurred for higher speeds (>180 rad/s). For the linear H-infinity controller, the risk of destabilization due to rotor contact with the clearance ring prevented a full set of results being obtained. Although light rubs resulted in limit-cycle response, sustained rubbing led to severe vibration requiring immediate controller shut down. Results for the base-level PD controller are also shown in Fig. 6b for comparison. Figure 7 shows orbit plots for a rotational speed of 95 rad/s for all three controllers. A limit cycle instability involving rub interaction with the clearance ring is evident for the linear H-infinity controller (Fig. 7c).

6. Conclusions

It has been shown how, for a rotordynamic model incorporating nonlinear effects, an H-infinity controller solution can be obtained by using numerical optimization to solve the HJI equation (in matrix inequality form). This leads to a suboptimal linear state feedback controller for the nonlinear rotordynamic system. For the test case investigated, controllers were designed to achieve rotor vibration suppression for a rotational frequency range including the first critical speed for rotor flexure. Although linear and nonlinear controllers had similar vibration suppression qualities over a low frequency range, linear designs were prone to lose stability during large amplitude vibration. The nonlinear H-infinity controller maintained stability while giving comparable vibration suppression qualities - when assessed by metrics used for the controller design optimization. Further work should develop the design approach for systems having more than one AMB and with rotordynamic models having multiple nonlinear terms, for example due to multiple clearance/backup bearings. This could validate the approach for typical AMB/rotor configurations and applications.

References

Abu-Khalaf, M., Huang, J., and Lewis, F.L. Nonlinear H2/H∞ Constrained Feedback Control, (2006), Springer-Verlag, London, ISBN: 1-84628-349-3.

Boyd, S., Feron, E., Ghaoui L. E.and Balakrishnan, V., Linear Matrix Inequalities in System and Control Theory, (1994), Pennsylvania: SIAM.

Cade I. S., Sahinkaya, M. N., Burrows, C. R. & Keogh, P. S. An active auxiliary bearing control strategy to reduce the onset of asynchronous periodic contact modes in rotor/magnetic bearing systems. Trans. ASME, J. Eng. Gas Turbines and Power, Vol. 132, (2010), Art. No. 052502.

Cole, M.O.T. and Keogh, P.S. Rotor vibration with auxiliary bearing contact in magnetic bearing systems, Part 2: Robust synchronous control to restore rotor position,' *Proc. Instn. Mech. Engrs, Part C, Journal of Mechanical Engineering Science*, Vol. 217, No. 4 (2003), pp. 393-409.

Chamroon, C., Cole, M.O.T. and Wongratanaphisan, T., An active vibration control strategy to prevent nonlinearly coupled rotor-stator whirl responses in multimode rotor-dynamic systems, IEEE Transactions on Control Systems Technology, Vol. 22, No. 3, (2014), pp. 1122-1129.

El-Shafai, A., Dimitri, A.S., Controlling journal bearing instability using active magnetic bearings, ASME J. Eng. Gas Turbines Power, Vol. 132, No. 1, (2010), art. no. 012502.

Inoue, T. Liu, J. Ishida Y. and Yoshimura, Y., Vibration control and unbalance estimation of a nonlinear rotor system using disturbance observer, ASME J. Vibr. Acoust., Vol. 131, (2009), Art. No. 031010.

Isidori, A. and Astolfi, A. Disturbance attenuation and H∞ control via measurement feedback in nonlinear systems, IEEE Transactions on Automatic Control, Vol. 37, No.9, (1992), pp. 1283-1293.

Karkoub, M. Robust control of the elastodynamic vibration of flexible rotor system with discontinuous friction, ASME J. Vib. Acoust., Vol. 133, (2011) art. no. 034501.

Schweitzer, G., Maslen, E. (Eds.), Magnetic Bearings: Theory, Design and Application to Rotating Machinery, Chapter 12, (2010), Springer, Berlin, ISBN: 978-3-642-00496-4.

Simon, A. and Flowers, G.T., Adaptive disturbance rejection and stabilisation for rotor system with internal damping, International Journal of Acoustics and Vibrations, Vol. 13, No. 2, (2008), pp. 73-81.

Sinha, P. K. and Pechev, A. N. Nonlinear H∞ controllers for electromagnetic suspension systems. IEEE Transactions on Automatic Control, Vol. 49, No. 4, (2004), pp. 563-568.

Van der Schaft, A.J. L2-Gain analysis of nonlinear systems and nonlinear state feedback H∞ control, IEEE Transactions on Automatic Control, Vol. 37, No. 6, (1992), pp. 770-784.

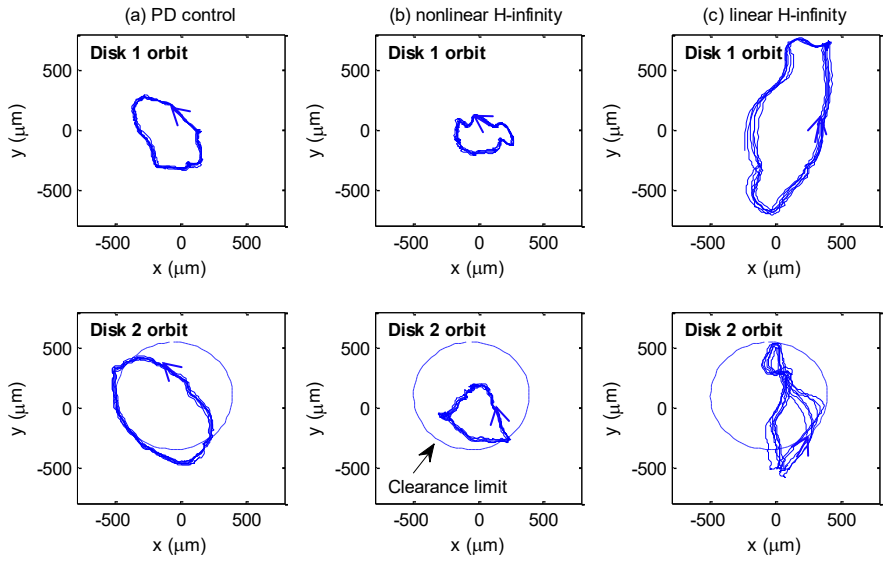

Fig. 7 Measured rotor orbits involving nonlinear rotor vibration for rotational speed of 95 rad/s